Electronic Supplementary Material (ESI) for Nanoscale.

SUPPLEMENTARY INFORMATION

Thermoplasmonic Enhancement of Upconversion in Small-Size Doped $NaGd(Y)F_4$ Nanoparticles Coupled to Gold Nanostars

Eduardo D. Martínez,[*,a] *Ricardo R. Urbano*[a] *and Carlos Rettori* [a,b]

[*] E-mail: edmartin@ifi.unicamp.br
[a] "Gleb Wataghin" Institute of Physics, University of Campinas, UNICAMP 13083-859, Campinas, SP, Brazil.
[b] CCNH, Federal University of ABC (UFABC), 09210-580, Santo André, SP, Brazil.

Contents

1 Optical set-up for upconversion measurements

Upconversion was studied by using a 976 nm, 900 mW Butterfly Laser, PM Fiber with FBG (Thorlabs Inc.). An aspheric and achromatic collimator (PAFA-X-4-B, ThorLabs Inc.) was used to collimate the laser beam. All measurements were performed at a nominal power of 500 mW, except otherwise indicated, controlled by a LDC210C laser diode controller (Thorlabs Inc.). The emission was analyzed with a QEPro spectrometer (Ocean Optics Inc.) coupled to an optical fiber of 600 µm diameter. A short-pass optical filter was used to avoid saturation of the spectrometer by the incident laser. Homogeneity of the sample was tested by measuring the emission in different points of the sample surface. The optical filter used to cut-off the laser light and the filtered corrected upconversion spectra are shown in Fig. S1. Although minor changes are observed for the emission spectra of UCNPs doped with Er^{3+}, for UCNPs doped with Tm^{3+} the correction of the spectra considering the transmittance of the optical filter clearly shows that the main emission line is that centered at 802 nm corresponding to the $^3H_4 \longrightarrow {}^3H_6$ transition.

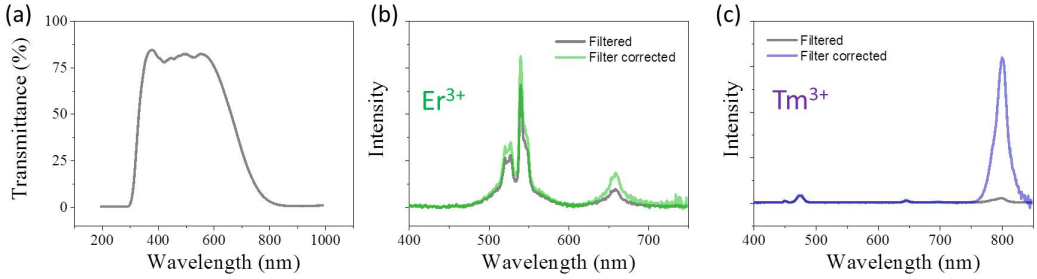

Figure S1 Filter correction of the emission spectra. (a) Optical transmittance of the applied filter. The acquired emission spectra and the filter corrected spectra are shown for UCNPs doped with (b) Er^{3+} and (c) Tm^{3+}.

2 Photothermal effect in AuNSs

A direct measurement of the increase of temperature of the AuNSs colloid was performed using a thermocouple. The results are shown in Fig. S2. Notice that the temperature profile in the cuvette is not homogeneous as heat is dissipated from regions along the path of the laser beam. This is easily seen in the control experiment using a pNIPAM solution in the absence of AuNSs, where the thermometer indicates 29 °C but the turbidity from the pNIPAM transition is already visible along the path of the laser beam (arrows), indicating in that region a temperature higher than the lower critical solubility temperature (LCST) of pNIPAM at 32 °C. This allows us to visualize this profile while the temperature reading critically depends on the exact position of the thermocouple.

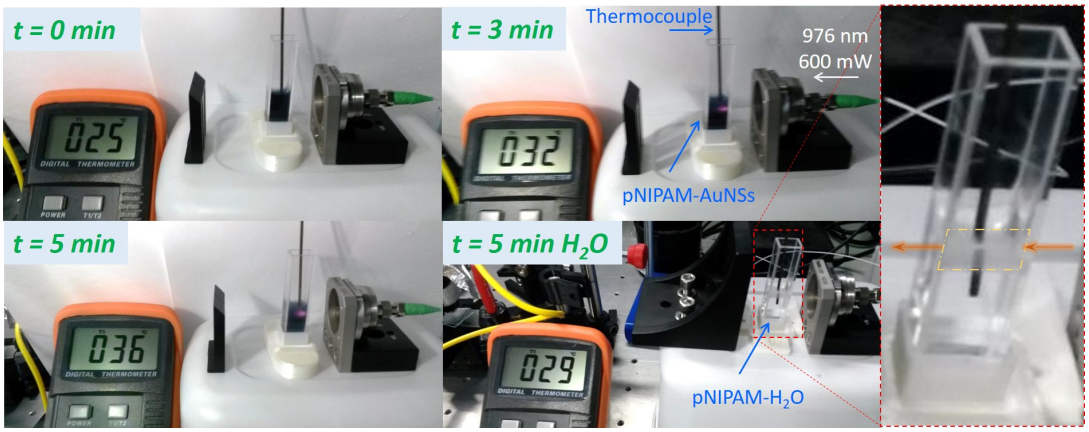

Figure S2 Photothermal effect in AuNSs colloids under irradiation with 976 nm collimated laser beam at 600 mW of nominal power. Temperature increase at different times probed by a thermocouple and by direct visualization of the LCST of pNIPAM.

3 Optical thermometry using UCNPs

Of particular interest is the temperature dependence of the ratio between different emission lines of Er^{3+} as it can be used for optical thermometry[1–3]. The thermometric parameter (Δ) can be defined as the ratio between the integrated intensity of the green emission bands of Er^{3+}, $^2H_{11/2} \longrightarrow {}^4I_{15/2}$ (H transition), and $^4S_{3/2} \longrightarrow {}^4I_{15/2}$ (S transition). A calibration was performed using large and small UCNPs deposited on silicon substrates and placed over a Peltier plate by using a thermally conductive paste. A thermocouple sensor was also placed in thermal contact to the Peltier plate. The emission spectra were acquired at different known temperatures and the thermometric parameter was calculated. In this way, a direct correlation between the thermometric parameter and the local temperature can be used to optically establish the temperature in each presented experiments. The calibration for each system is presented in Fig. S3.

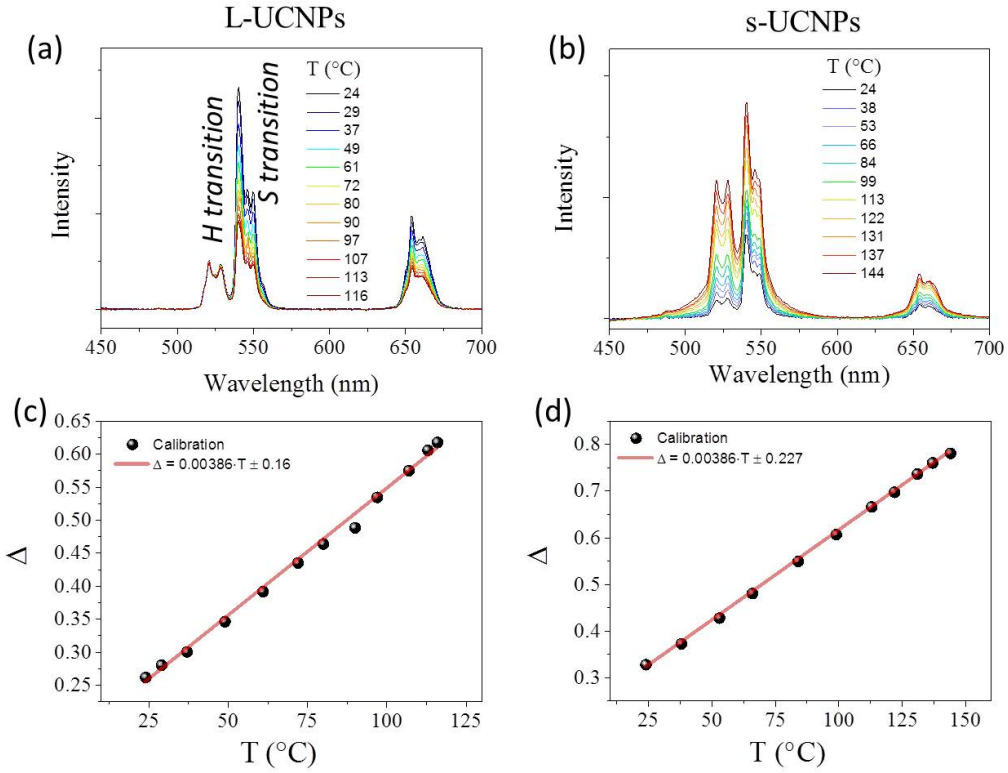

Figure S3 Calibration for the optical thermometry by using the normalized ratio of the H and S transitions of Er^{3+}. The thermometric parameter (Δ) was calculated at different known temperatures using (a) L-UCNPs and (b) s-UCNPs.

4 Power dependence of the upconverted emission

The emissions produced from the different systems studied when exposed with infrared laser light at various nominal powers provide insights into the underlying mechanisms involved. For UCNPs doped with Er^{3+} in the presence or absence of AuNSs was presented and discussed in the main text. Here, we provide additional information regarding the s-UCNPs doped with Tm^{3+} (Fig. S4a) where, again, a higher exponent in the power-law is obtained in the presence of AuNSs (Fig. S4b). Also, the calculated local temperatures at each pump-power for small and large UCNPs doped with Er^{3+} is shown in Fig. S4c,d exposing the heating effect of the laser light and the major photothermal effect due to the AuNSs.

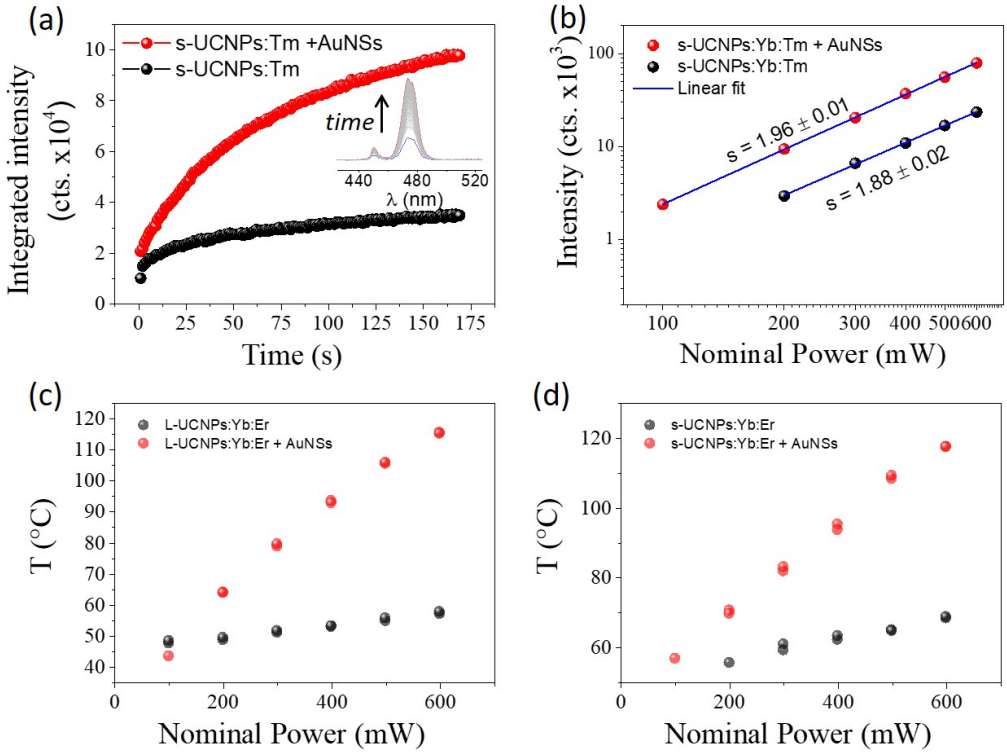

Figure S4 Evolution of (a) the emission intensity (500 mW, Δt=1 s) and (b) power-law dependence in s-UCNPs doped with Tm^{3+}. Temperature of the emitting UCNPs when excited at different pump powers in the presence or absence of AuNSs for (c) L-UCNPs and (d) s-UCNPs doped with Er^{3+}.

5 Characterization of the UCNPs-AuNSs bilayer structures

The correct comparison of the emission intensity and the thermal effects of samples containing small or large UCNPs demands a complete characterization of the homogeneity and thickness of the comprising layers. To evaluate this issue, stylus profilometry was performed on the AuNSs and UCNPs layers by making a scratch. We focused on regions close to the edge of the AuNSs patch, where the luminescence measurement were actually performed. Results are shown in Fig. S5. As a first difference, the layer containing s-UCNPs was measured to be 0.2 μm thick, while the thickness of the bilayer formed by s-UCNPs on top of the AuNSs was measured to be 1.5±0.5 μm. This corresponds to a thickness of roughly 1.3 μm for the AuNSs patch. On the other hand, the sample containing L-UCNPs (hexagonal plates 300 nm x 160 nm) was formed by dispersed nanoparticles uniformly covering the sample. However, in this case the thickness of the AuNSs patch was measured to be around 1.0 μm, meaning that there is a smaller amount of AuNSs. No clear profiles were obtained for L-UCNPs deposited outside the AuNSs patch. In our understanding, both the higher scattering properties of L-UCNPs and the fewer AuNSs explain the lower temperature reached with L-UCNPs.

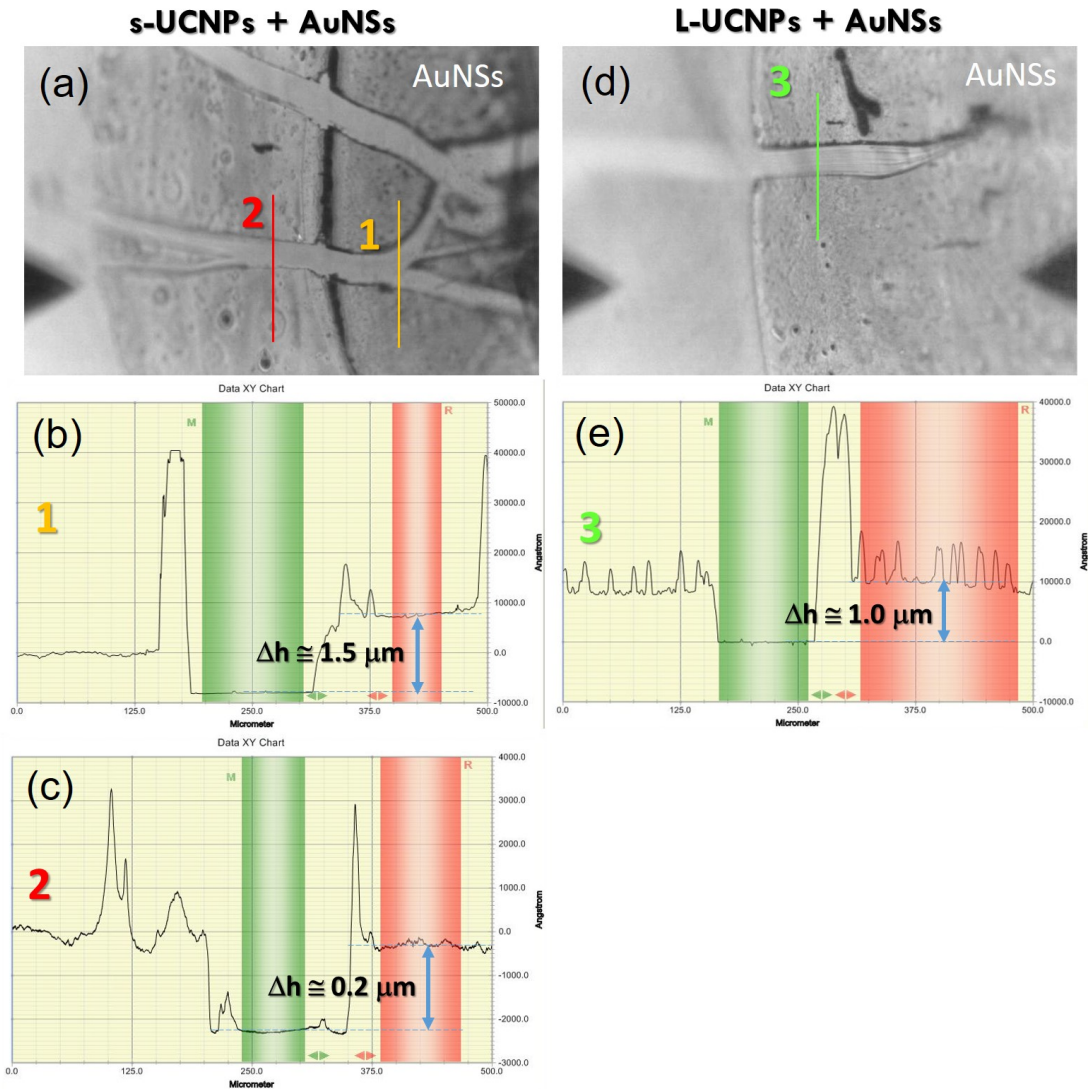

Figure S5 Stylus profilometry measurements of samples formed by AuNSs and (a-c) s-UCNPs or (d, e) L-UCNPs. The paths of the profilometry scans are shown as straight lines: line 1 lies inside the region containing s-UCNPs deposited on AuNSs while line 2 scans only the s-UCNPs layer. Line 3 indicates the profile in the AuNSs region covered by L-UCNPs. The indicated thicknesses (Δh) were calculated as a difference in the average values of height in regions highlighted in green and red.

To compare the emission intensity of upconversion nanoparticles with and without Au nanostars, we acquired optical microscopy images and performed AFM measurements in both regions for comparison (Fig. S6). Furthermore, we directly captured the upconversion emissions by an optical microscope, allowing us to compare the density of UCNPs in each region and their emission intensity. In particular, Figs. S6i-l show that the emission centers are evenly distributed in the regions with and without AuNSs but the intensity of the emissions is strongly affected by the presence of AuNSs, being quenched for L-UCNPs and enhanced for s-UCNPs. Therefore, the mentioned changes of emission intensity are not due to the amount of particles. In addition, the slow kinetics of the enhancement (Fig. 4d and S4a) and its correlation with the temperature-size-dependent emissions

(Figs. 3d-f, main text) point out to a thermally induced effect.

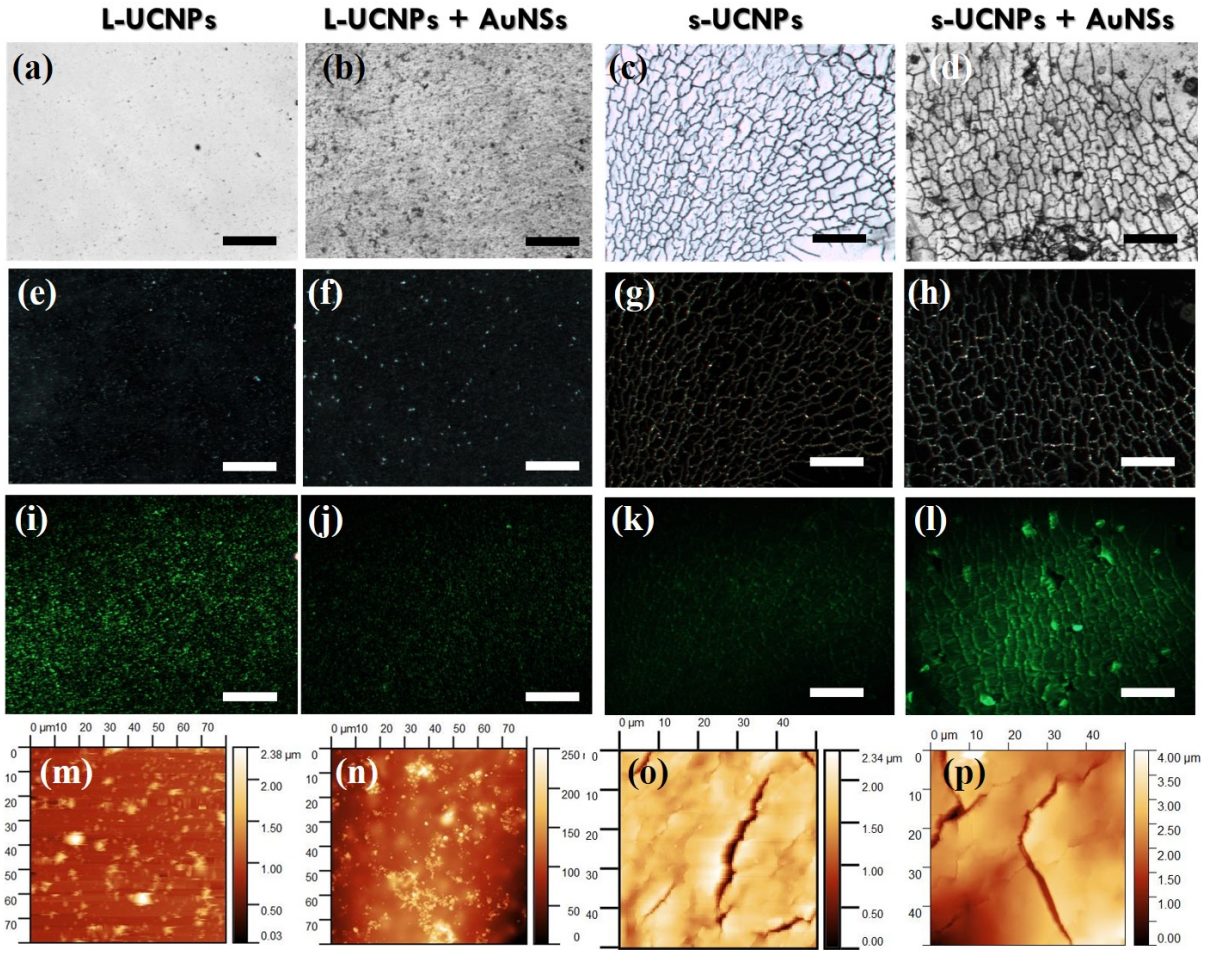

Figure S6 Characterization of the surface covered by UCNPs in regions with and without AuNSs. Optical images were acquired in (a-d) bright field mode, (e-h) dark field mode and (i-l) under 976 nm, 500 mW. The scale bar is 200 µm in all cases. AFM images were obtained by scanning square areas of (m, n) 80 µm and (o, p) 50 µm, respectively.

6 Details on the electronic transitions involved in the upconversion

The energy levels of the Yb^{3+}/Er^{3+} and Yb^{3+}/Tm^{3+} systems are presented in Fig. S7 together with the electronic transitions and energy transfer from the sensitizer to the activator.

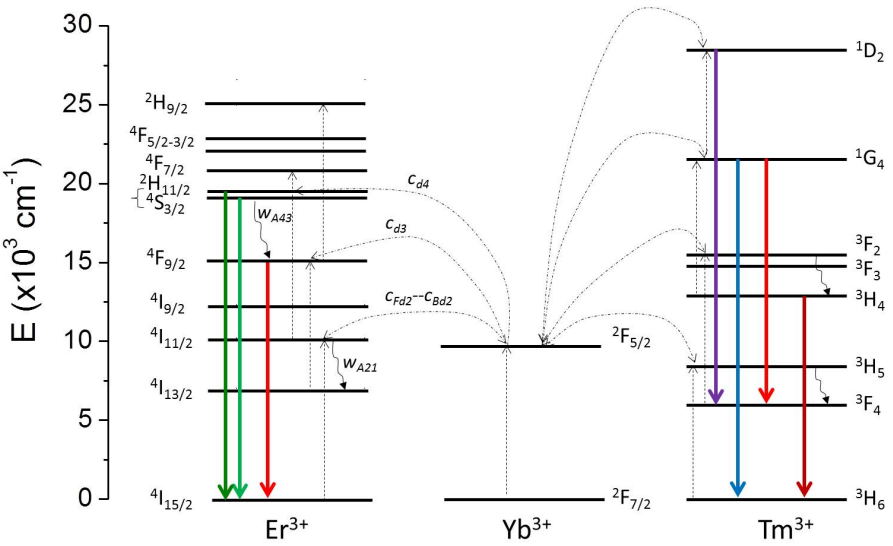

Figure S7 Schematic illustration of the energy transfer upconversion mechanism detailing the energy levels of donor (Yb^{3+}) and acceptors (Er^{3+}) and (Tm^{3+}) dopants present in UCNPs.

References

[1] C. D. S. Brites, P. P. Lima, N. J. O. Silva, A. Millán, V. S. Amaral, F. Palacio and L. D. Carlos, *New J. Chem.*, 2011, **35**, 1177.

[2] C. D. S. Brites, A. Millán and L. D. Carlos, *Handb. Phys. Chem. Rare Earths*, 2016, **49**, 339–427.

[3] S. Balabhadra, M. L. Debasu, C. D. S. Brites, R. A. S. Ferreira and L. D. Carlos, *J. Phys. Chem. C*, 2017, **121**, 13962–13968.